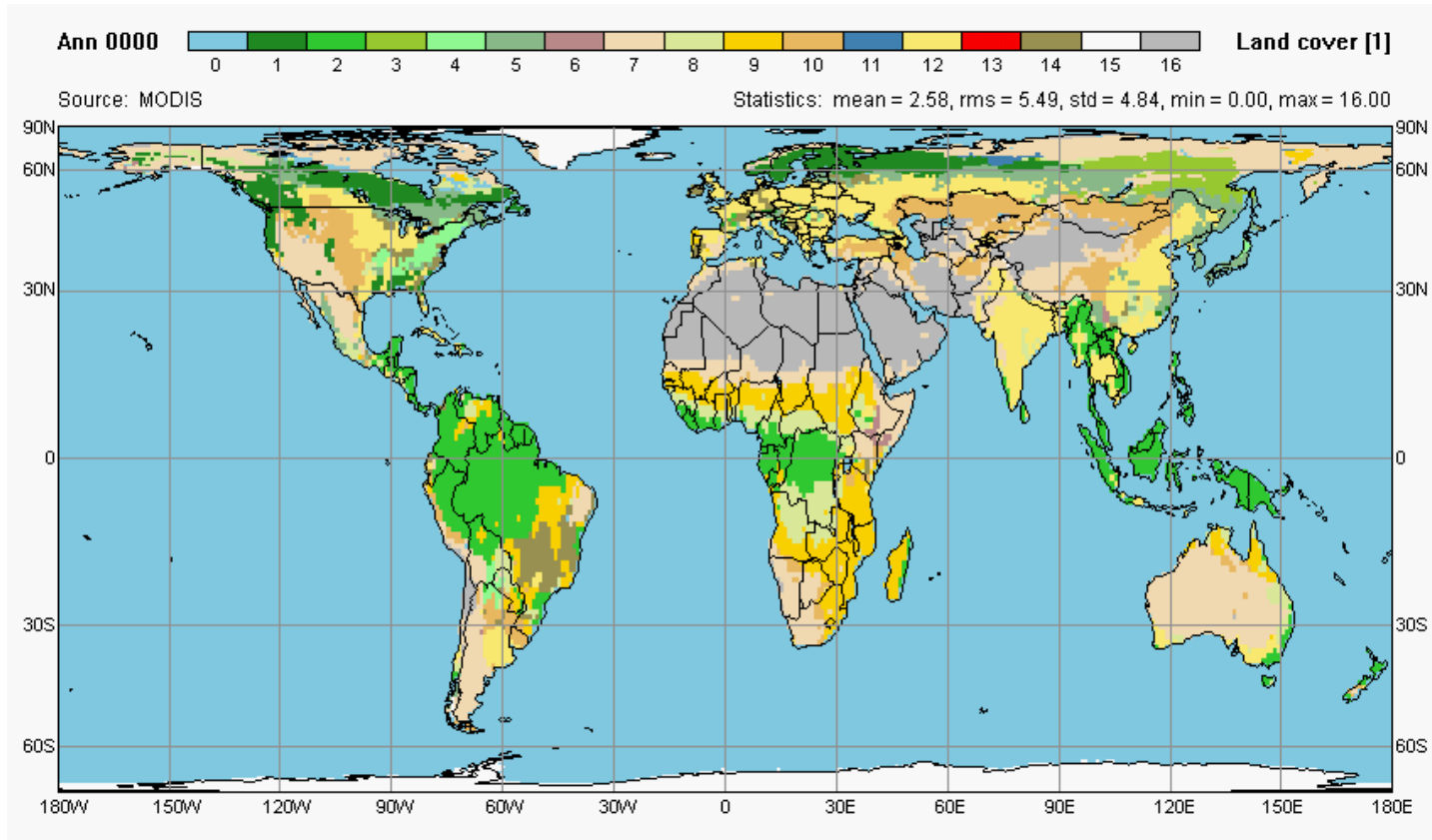


# Terrestrial Biomes



**Fig. 12.3** Contemporary global land cover derived from a MODIS data set [02Fri]. 17 land cover types are distinguished, according to the IGBP classification: 0, water bodies; 1, evergreen needleleaf forests; 2, evergreen broadleaf forests; 3, deciduous needleleaf forests; 4, deciduous broadleaf forests; 5, mixed forests; 6, closed shrublands; 7, open shrublands; 8 woody savannas; 9, savannas; 10, grasslands; 11, permanent wetlands; 12; croplands; 13, urban and built-up; 14, cropland/natural vegetation mosaic; 15, snow and ice; 16, barren or sparsely vegetated.

Diese und einige der folgenden Abbildungen stammen aus: Gerten et al., 2005, Terrestrial Carbon and Water Fluxes. In: Hantel., M. (Ed.), Observed Global Climate, *Landold-Börnstein*, V/6 (Geophysics/Climatology), Springer

# The importance of terrestrial biomes: the global water cycle

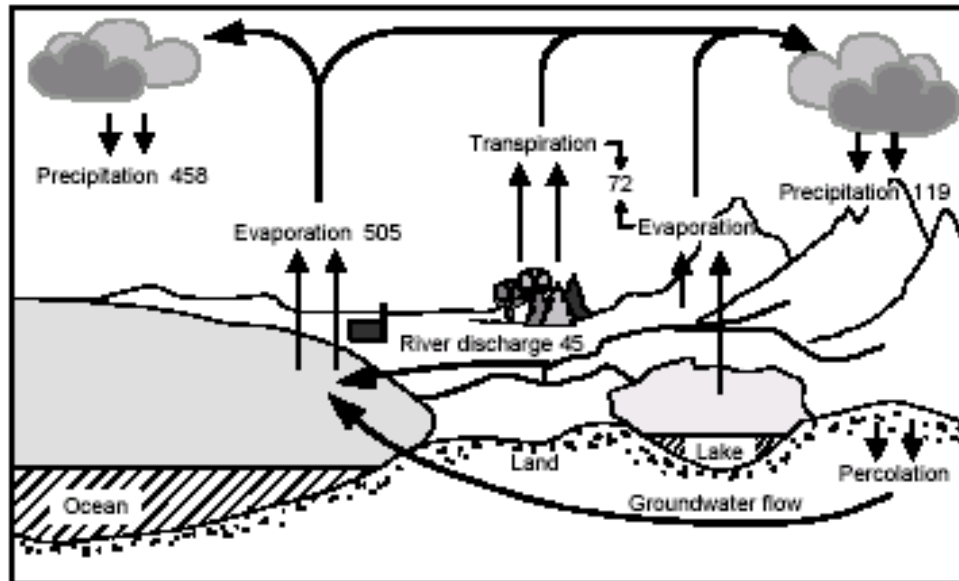


Fig. 12.1 Scheme of the global water cycle with flux components, and estimates of their annual means [ $1,000 \text{ km}^3 \text{ yr}^{-1}$ ] (estimates after [78Kor]).

Gerten et al. (2005)

Plants exert a strong control on the flow of water from the land masses into the atmosphere. They tend to maintain an optimal balance between limitation of  $\text{H}_2\text{O}$  loss and admission of  $\text{CO}_2$ , thus influencing the release and uptake of the two most important greenhouse gases. Under stress (in particular water stress), the stomata close and carbon uptake is reduced or ceases.

# Water reservoirs

**Table 12.1.** Water storages on the earth and residence times (after [78Kor]).

Component of the hydrosphere	Volume [1,000 km <sup>3</sup> ]	Percentage of total water [%]	Percentage of total fresh water [%]	Residence time
Oceans	1,338,000	96.54	0	2,500 yr
Ground water	23,400	1.688	30.06 <sup>1)</sup>	1,400 yr
Soil moisture	16.5	0.001	0.047	1 yr
Permanent ice	24,364	1.758	69.56	1,600-10,000 yr
Lakes	176.4	0.0127	0.26 <sup>1)</sup>	17 yr
Swamps	11.5	0.0008	0.03	5 yr
Rivers	2.1	0.0002	0.006	16 d
Biological water	1.1	0.0001	0.003	Several h
Atmosphere	12.9	0.0009	0.037	8 d
Total water	1,385,984.5	100	0	--
Total fresh water	35,029	2.53	100	--

<sup>1)</sup> Only fresh water part of specific volume considered.

Gerten et al. (2005)

# Soil water availability

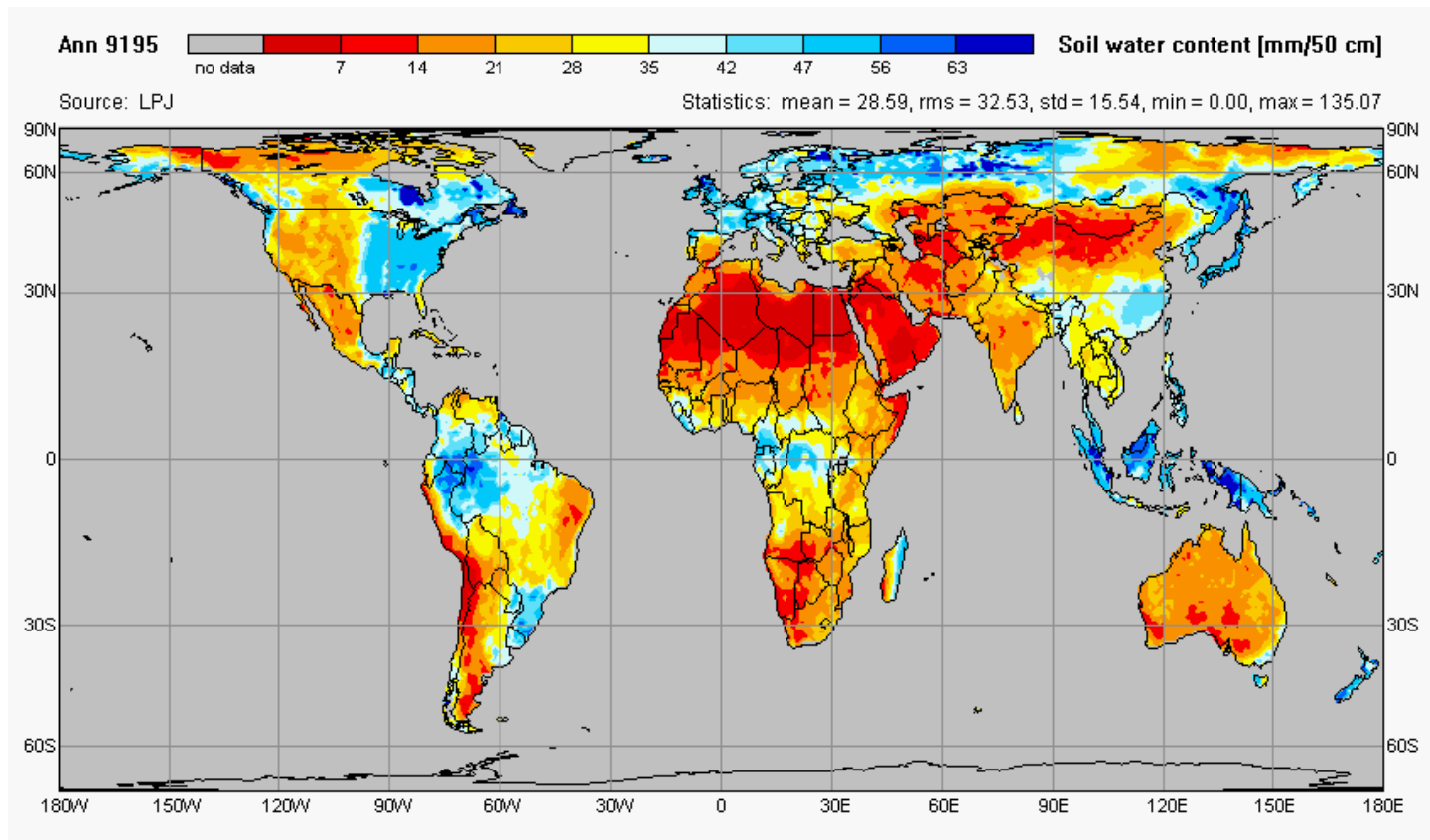


**Fig. 12.5** 1991-1995 mean global soil moisture [ $\text{mm } 0.5\text{m}^{-1}$ ] simulated by the LPJ model for the upper 50 cm of the soil column.

Gerten et al. (2005)

# Actual evapotranspiration

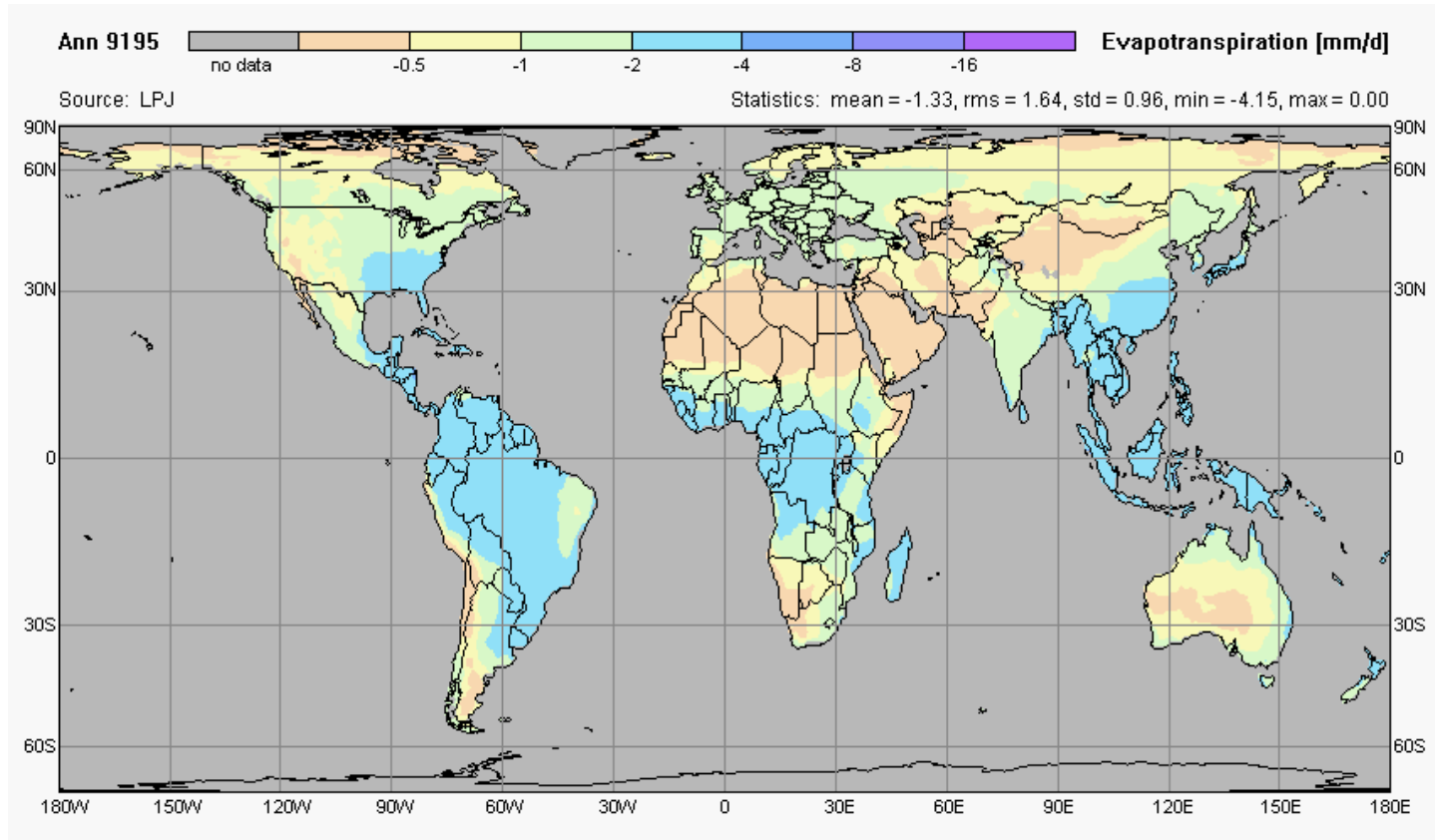
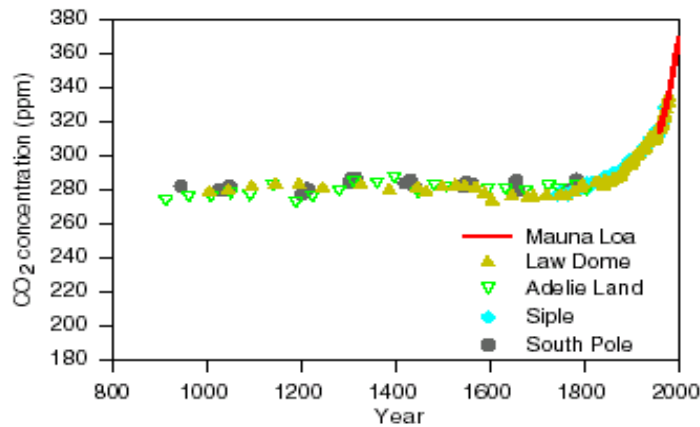


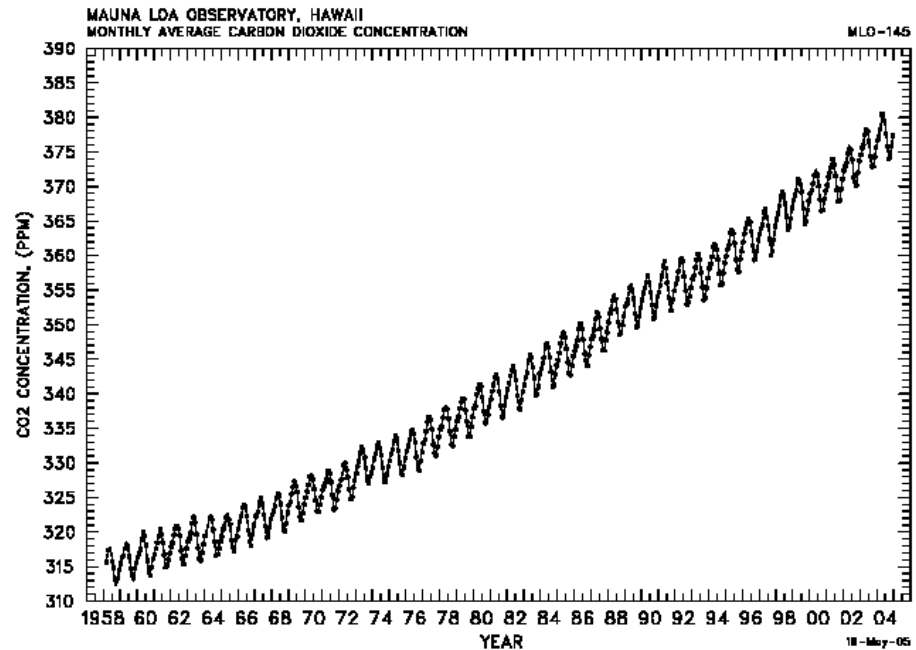
Fig. 12.6 1991-1995 mean actual evapotranspiration [mm d<sup>-1</sup>], simulated by the LPJ model.

Gerten et al. (2005)

# The importance of terrestrial biomes: atmospheric CO<sub>2</sub>

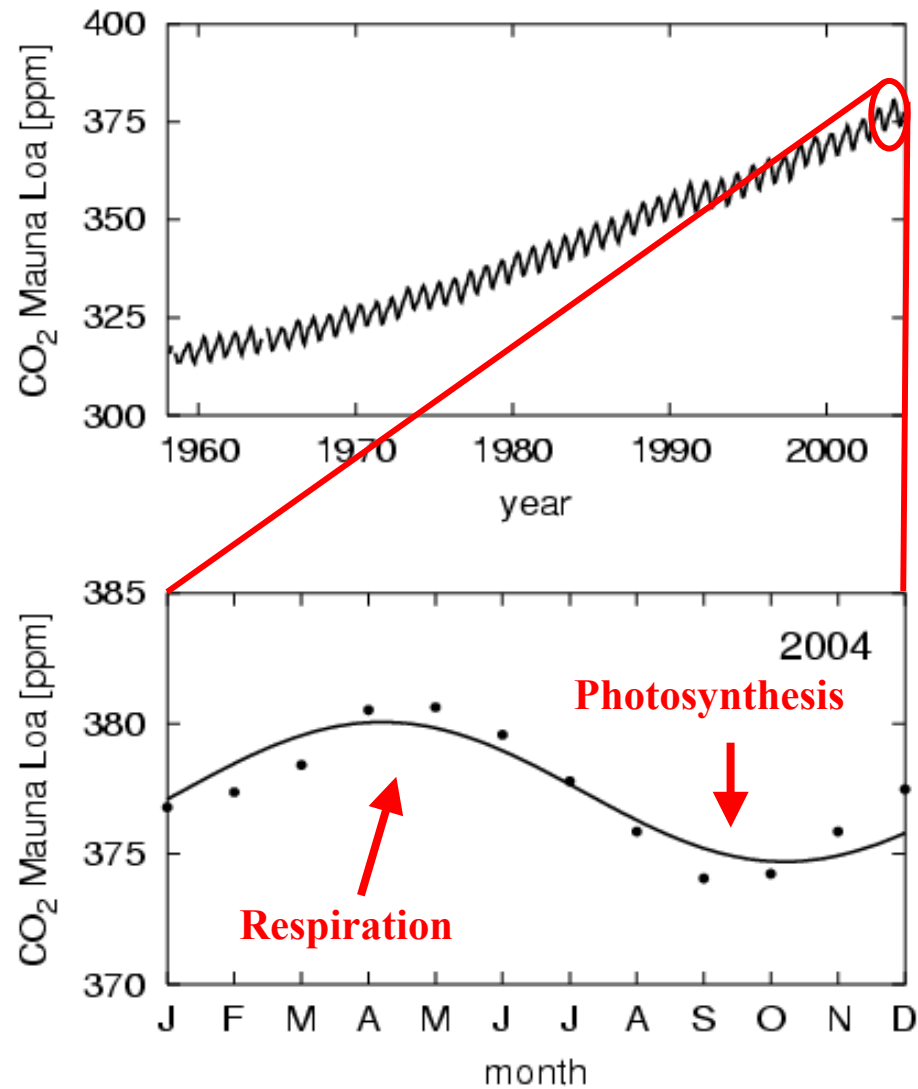


IPCC (2001)  
[www.ipcc.ch](http://www.ipcc.ch)



TRENDS (2005)  
[cdiac.ornl.gov/trends/co2/sio-mlo.htm](http://cdiac.ornl.gov/trends/co2/sio-mlo.htm)

# Atmospheric CO<sub>2</sub>



TRENDS (2005)



## Terrestrial biomes in the course of the seasons

In the extratropics, the activity of terrestrial biomes undergoes a seasonal cycle. This can be monitored from space, because the spectrum of radiation reflected by foliage has a different shape from the spectrum for all types of soils (Monteith and Unsworth, 1990).

Denoting with  $\rho_{\text{VIS}}$  and  $\rho_{\text{NIR}}$  the reflectivity of leaves in the visible (VIS) and near infrared (NIR) range of the spectrum, we can define the so-called normalized difference vegetation index (NDVI) as:

$$\text{NDVI} = \frac{\rho_{\text{NIR}} - \rho_{\text{VIS}}}{\rho_{\text{NIR}} + \rho_{\text{VIS}}}$$

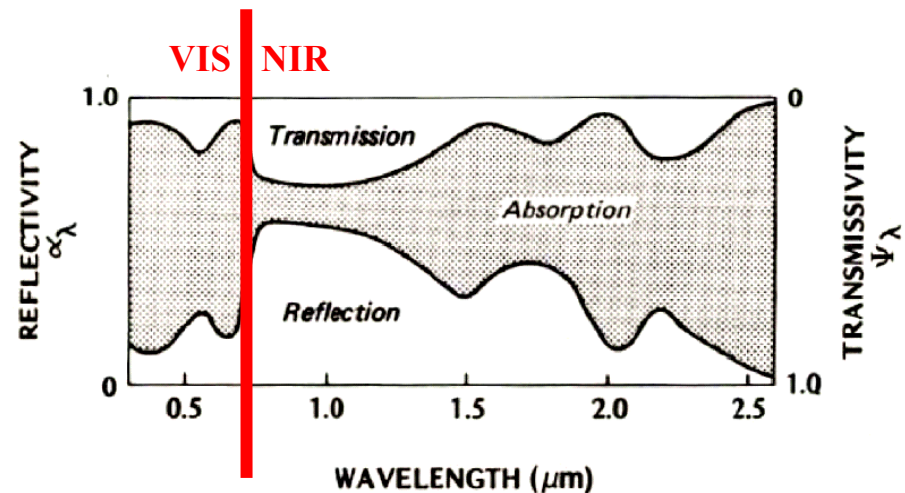


Figure 4.4 Idealized relation between wavelength and the reflectivity ( $\alpha$ ), transmissivity ( $\Psi$ ) and absorptivity ( $\zeta$ ) of a green leaf (after Monteith, 1965a).



## Using the NDVI

The usefulness of the NDVI resides in the fact that it is related to properties of the vegetation such as the fraction of photosynthetic active radiation absorbed by the leaves (FPAR), the leaf-area index (LAI) or the roughness length ( $z_0$ ).

Algorithms for retrieving vegetation properties from measurements of the NDVI are reviewed by Stöckli and Vidale (2004)

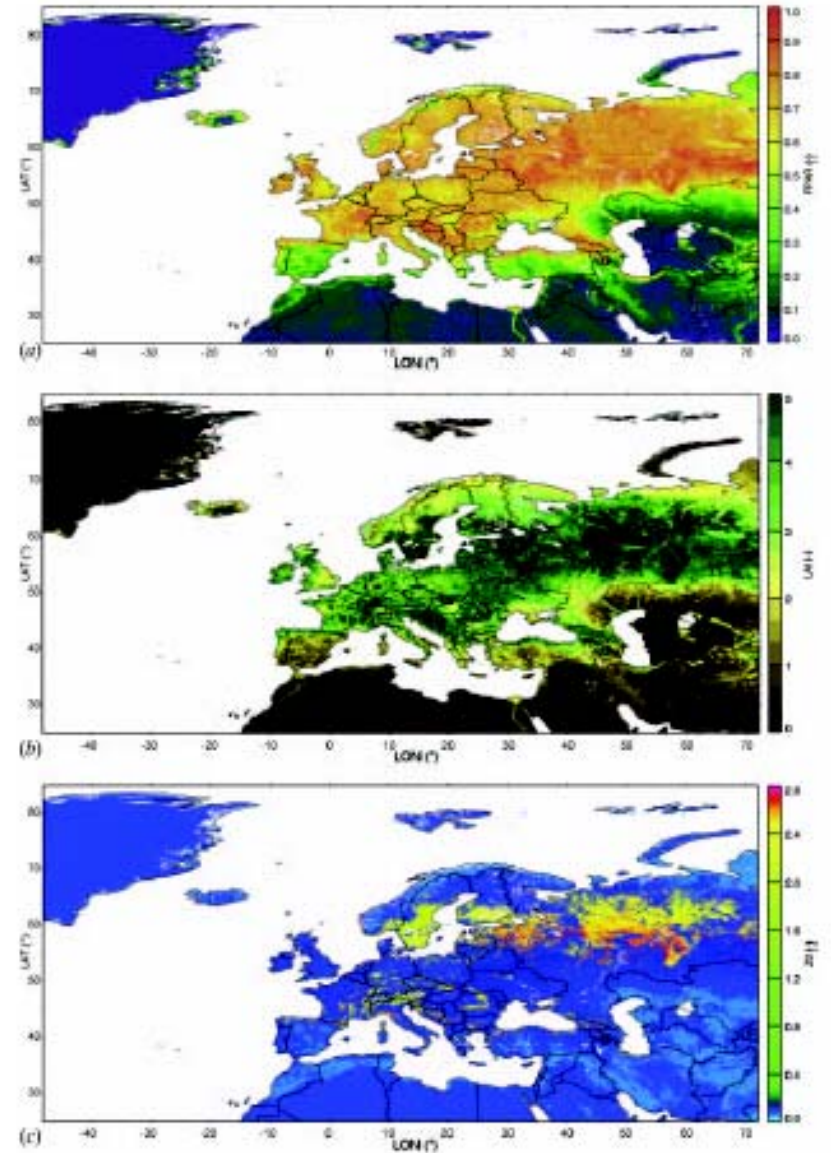


Figure 6. Maps of the derived land surface parameters covering the period from 10 to 21 July (average yearly climatology derived from the years 1982–2001). (a) FPAR, (b) LAI and (c)  $z_0$ .

# Monitoring the NDVI

As shown e.g. by Stöckli and Vidale (2004)\*, with the available data it is currently possible to reconstruct with some confidence a 20-years long record of the NDVI. Examples for Europe are discussed in the original paper.

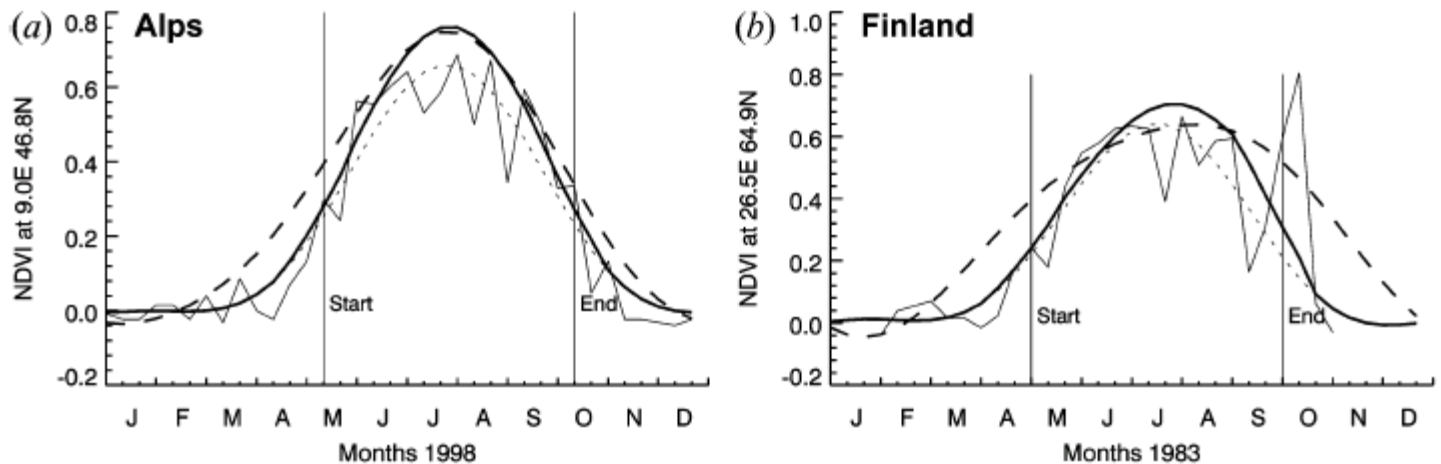


Figure 1. Pathfinder NDVI time-series (thin solid), Fourier adjusted with an unweighted scheme (dotted), weighted after Sellers *et al.* (1996b) (dashed) and with the EFAL-NDVI method discussed in this paper (thick solid). (a) Swiss Alps, (b) Finland, (c) Norway, (d) Finland, (e) north-west France, (f) Sicily, (g) Ireland, and (h) Sweden.

\* Stöckli, R. and P. Vidale, 2004, European plant phenology and climate as seen in a 20-year AVHRR land-surface parameter dataset, *INT. J. REMOTE SENSING*, VOL. 25, NO. 17, 3303–3330.

# Temporal variability of the NDVI

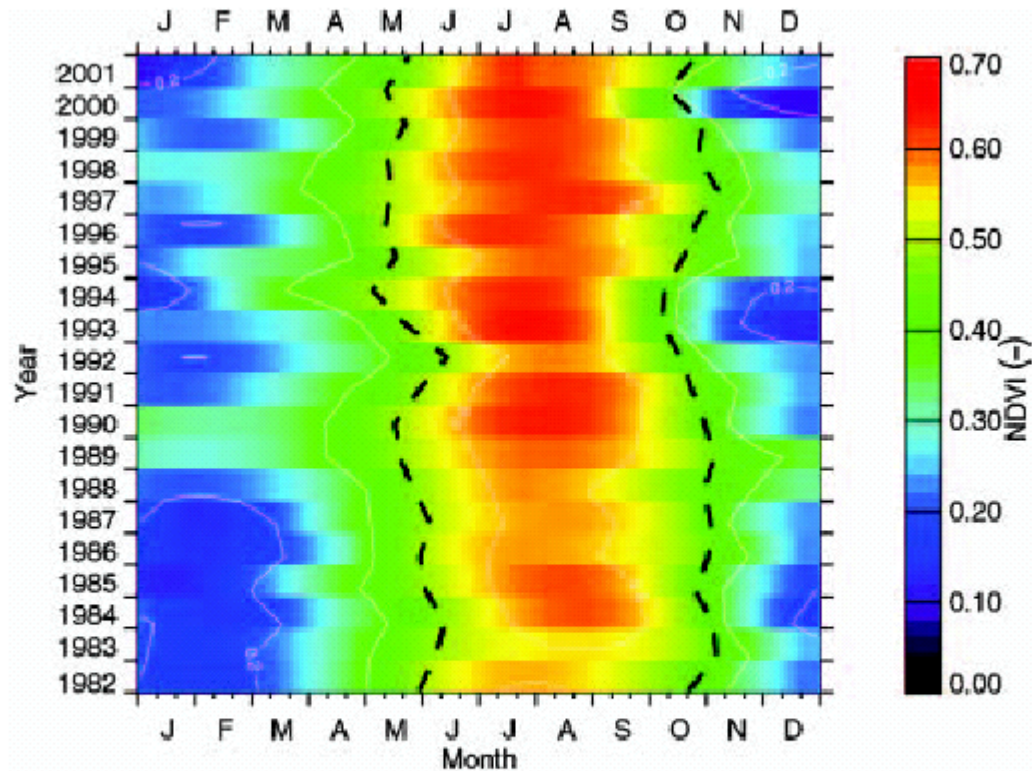
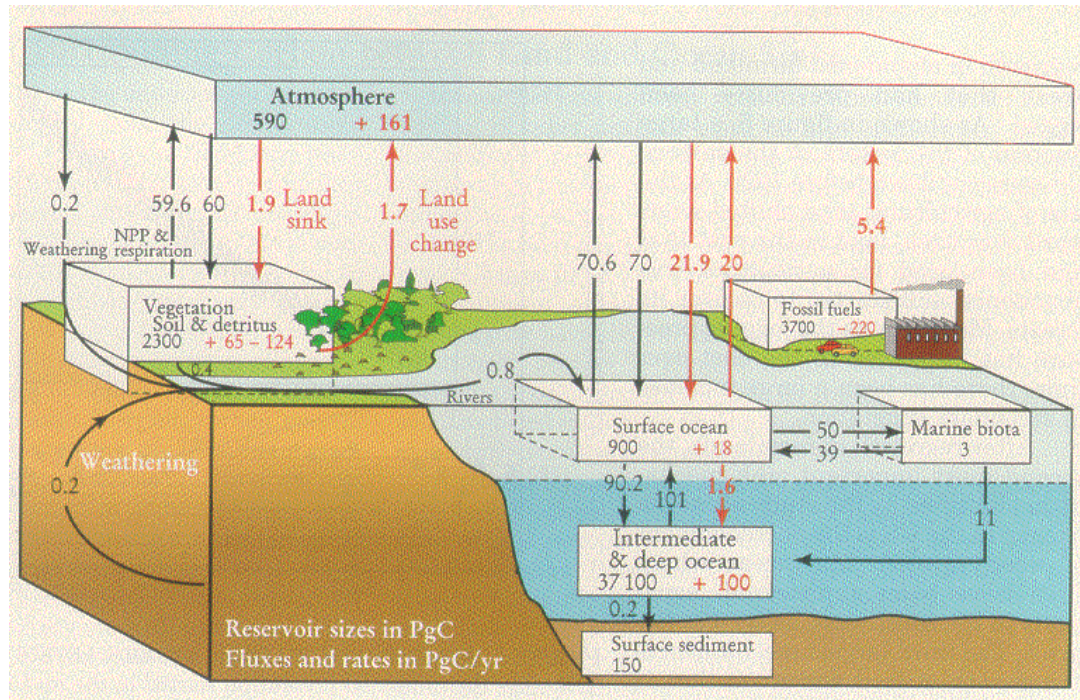


Figure 9. Interannual and seasonal variability as observed in the 20-year period from 1982 to 2001 for the Alps sub-domain. The area-averaged start and end of the growing season is plotted as a black dashed line.

Stöckli and Vidale (2004)

# The importance of terrestrial biomes: the global carbon cycle

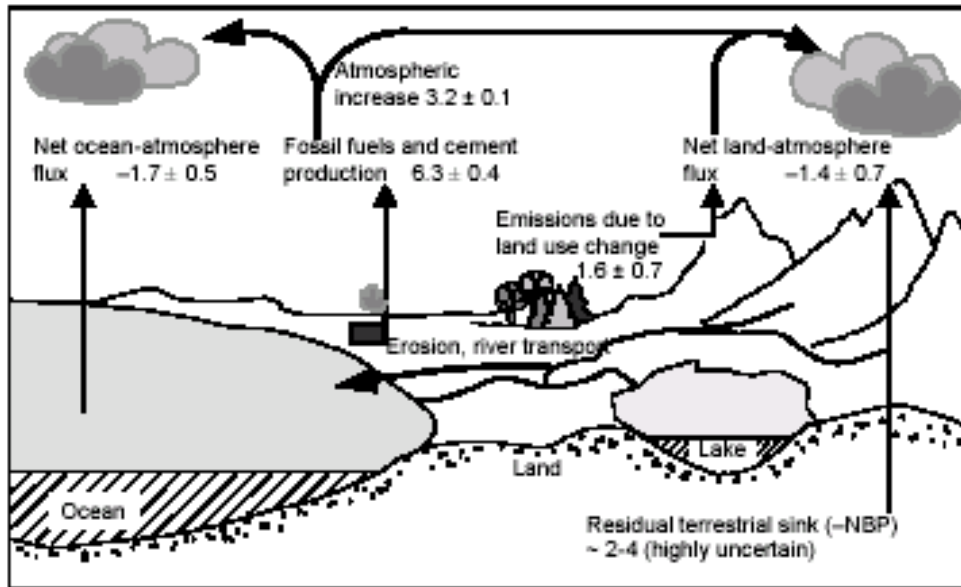


**FIGURE 1. GLOBAL CARBON CYCLE.** Arrows show the fluxes (in petagrams of carbon per year) between the atmosphere and its two primary sinks, the land and the ocean, averaged over the 1980s. Anthropogenic fluxes are in red; natural fluxes in black. The net flux between reservoirs is balanced for natural processes but not for the anthropogenic fluxes. Within the boxes, black numbers give the preindustrial sizes of the reservoirs and red numbers denote the changes resulting from human activities since preindustrial times. For the land sink, the first red number is an inferred terrestrial land sink whose origin is speculative; the second one is the decrease due to deforestation.<sup>16</sup> Numbers are slight modifications of those published by the Intergovernmental Panel on Climate Change.<sup>3</sup> NPP is net primary production.

Sarmiento and Gruber (2002)

1 Pg (petagram)  $\equiv 10^{15}$  g  $\equiv 10^{12}$  kg

# The global carbon cycle



Gerten et al. (2005)

Fig. 12.2 Scheme of the main compartments of the global carbon cycle, and estimated carbon fluxes for 1990-1999 [Gt C yr<sup>-1</sup>] based on atmospheric observations of CO<sub>2</sub> and O<sub>2</sub> (from [01Sch]). Negative signs indicate net sinks, i.e., a net flux from the atmosphere to ocean or land. According to a recent revision, the magnitude of the net land-atmosphere flux is lower by a factor of two, while the ocean-atmosphere flux is higher by the same amount [02Pla].

**Table 12.2.** Contemporary carbon storage in the major reservoirs of the earth (after [00Fal]). Note that the figures are approximate.

Pools	Quantity [Gt]
Atmosphere	720
Oceans	38,400
Lithosphere (sedimentary carbonates, kerogens)	>75,000,000
Terrestrial biosphere (total)	2,000
Living biomass	800
Dead biomass	1,200
Aquatic biosphere	1.5
Fossil fuels (coal, oil, gas, peat)	4,130

# Carbon reservoirs in terrestrial biomes

With the exception of the tropical rain forests, in all other terrestrial biomes the largest amount of C is stored in the soil.

Biom	Fläche (10 <sup>6</sup> km <sup>2</sup> )	Kohlenstoffvorrat (Gt C)		
		Vegetation	Boden	Total
Tropische Wälder	17,6	212	216	428
Temperierte Wälder	10,4	59	100	159
Boreale Wälder	13,7	88	471	559
Savannen	22,5	66	264	330
Temperierte Grasländer	12,5	9	295	304
Wüsten & Halbwüsten	45,5	8	191	199
Tundra	9,5	6	121	127
Feuchtgebiete	3,5	15	225	240
Landwirtschaft	16	3	128	131
<b>Total</b>	<b>151,2</b>	<b>466</b>	<b>2011</b>	<b>2477</b>

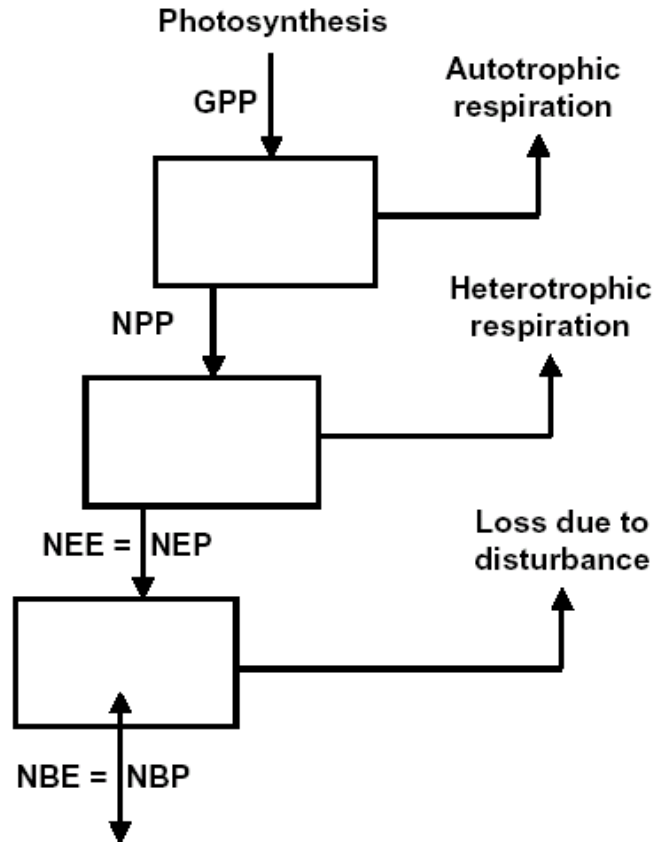
Wolfgang Cramer (2005)

$$2011 / 466 \sim \underline{5}$$

1 Gt C  $\equiv$  10<sup>12</sup> kg C  $\equiv$  10<sup>15</sup> g C (1 Pg)

# Some definitions

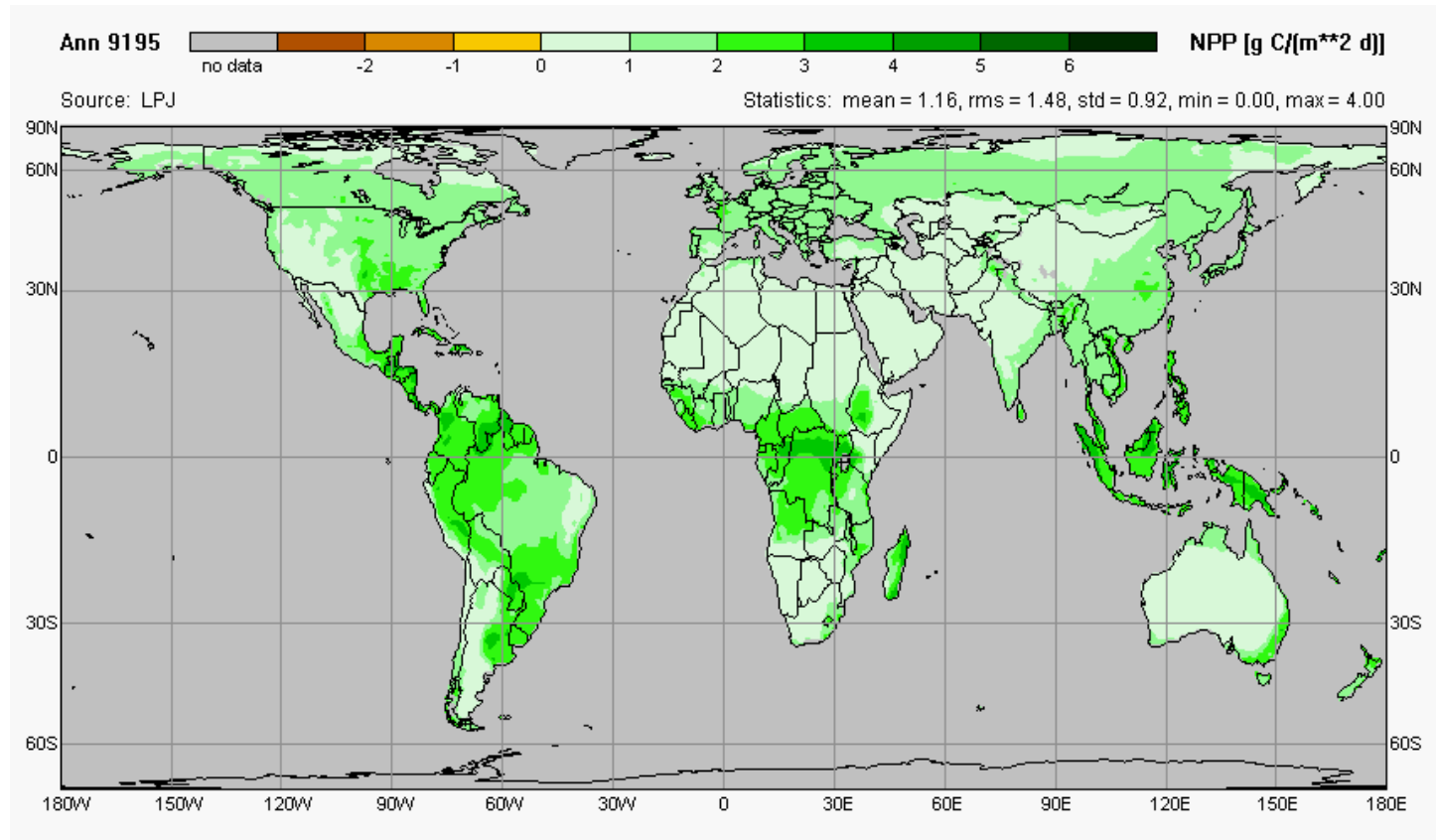
**Figure 2:** Diagrammatic representation of the main terms describing system carbon balances. Arrows indicate that GPP and NPP are always positive (carbon gains by the system), NEE is usually, but not always, positive, and NBE can be positive or negative.



Kirschbaum et al. (2002)

- **GPP:** gross primary production, the total amount of C fixed by plants through photosynthesis. Globally GPP  $\sim 120 \text{ Gt yr}^{-1}$ ;
- **NPP:** net primary production, i.e. GPP minus autotrophic respiration. Globally NPP  $\sim 60 \text{ Gt yr}^{-1}$ ;
- **NEE or NEP:** net ecosystem exchange or net ecosystem production, i.e. NPP minus heterotrophic respiration. Globally NEE/NEP  $\sim 10 \text{ Gt yr}^{-1}$ ;
- **NBE or NBP:** net biome exchange or net biome production, NEE or NEP minus the losses due to disturbances (fires, soil tillage, ...). Globally NBE/NBP  $\sim +1 \text{ Gt yr}^{-1}$ .

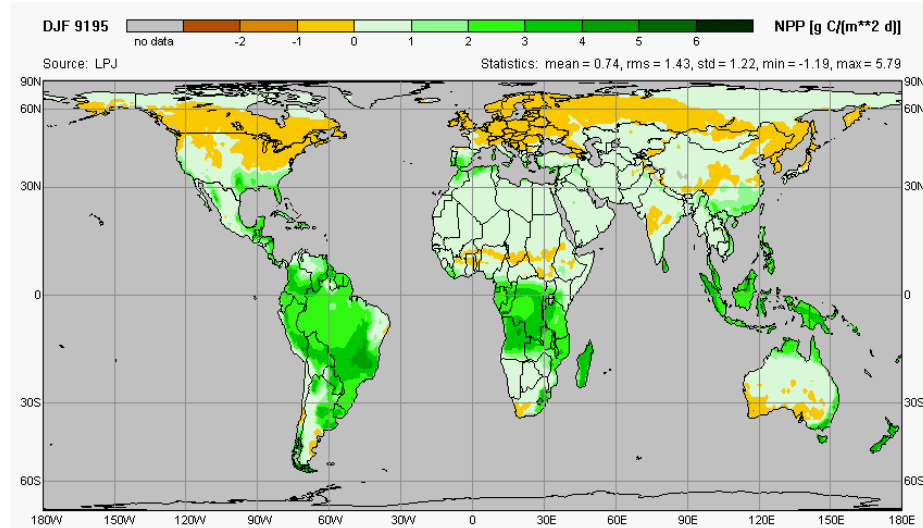
# Worldwide distribution of NPP [g C m<sup>-2</sup> d<sup>-1</sup>]: annual mean values



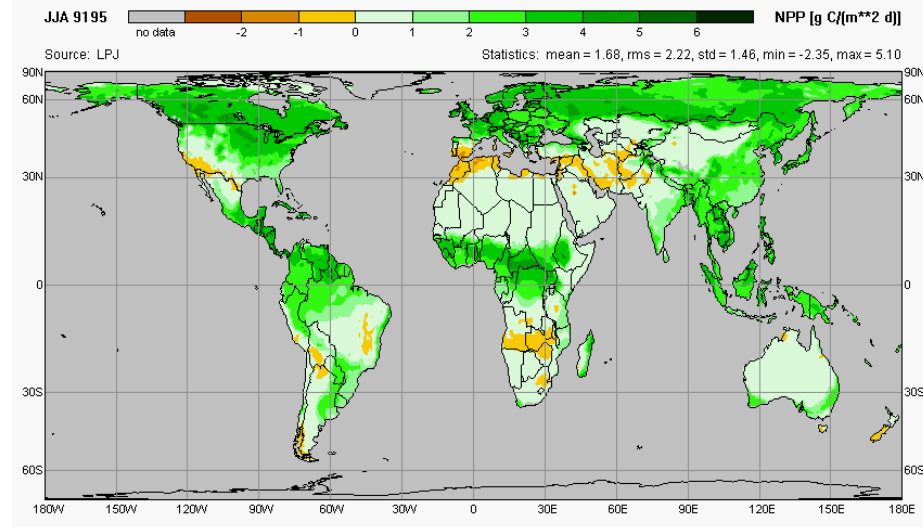
This and the following pictures were obtained from simulations with the Lund-Potsdam-Jena (LPJ) model.

# Worldwide distribution of NPP [g C m<sup>-2</sup> d<sup>-1</sup>]: seasonal mean values

Dec-Jan-Feb

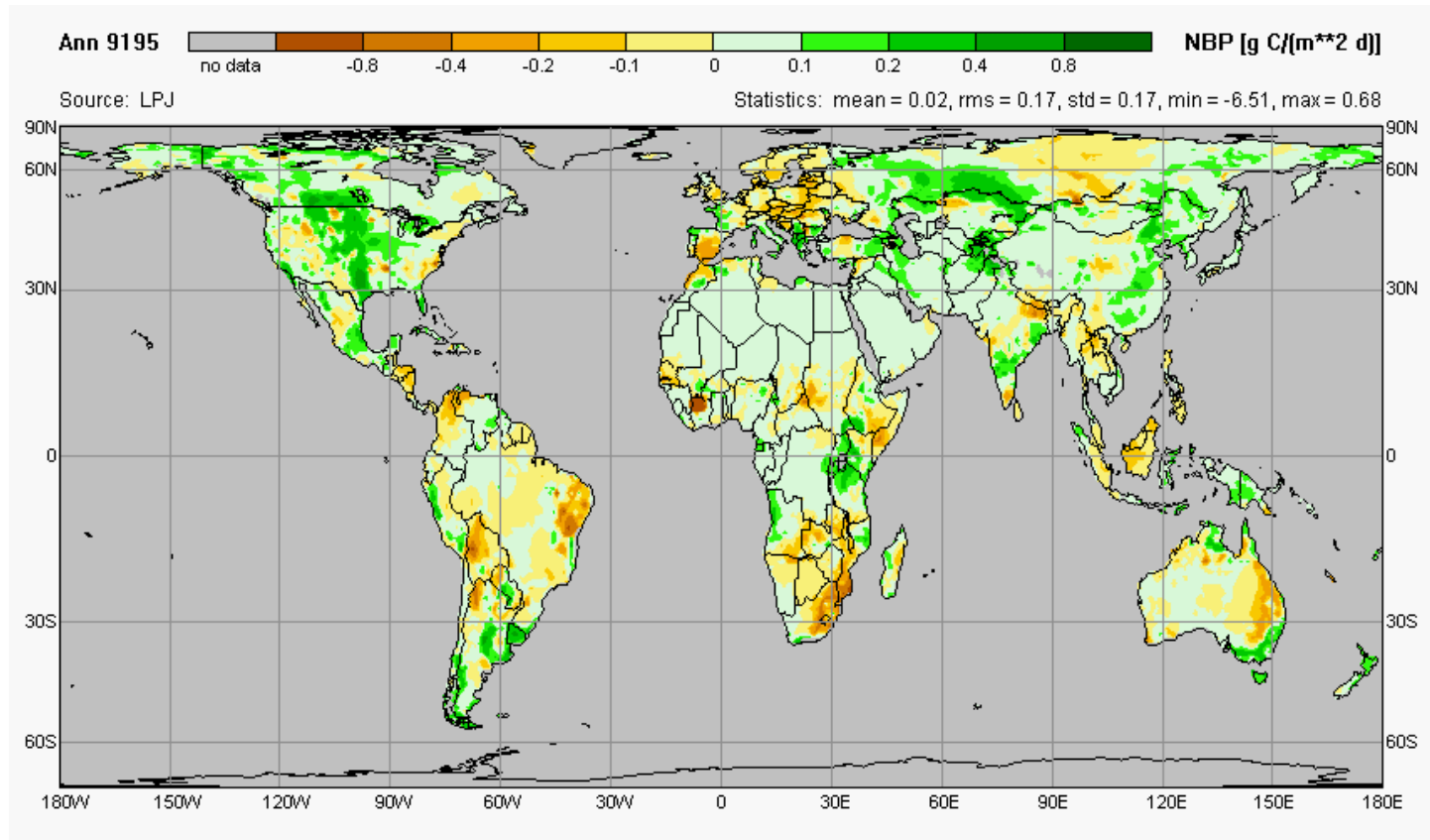


Jun-Jul-Aug



Gerten et al. (2005)

# Worldwide distribution of NBP [g C m<sup>-2</sup> d<sup>-1</sup> ]: annual mean values

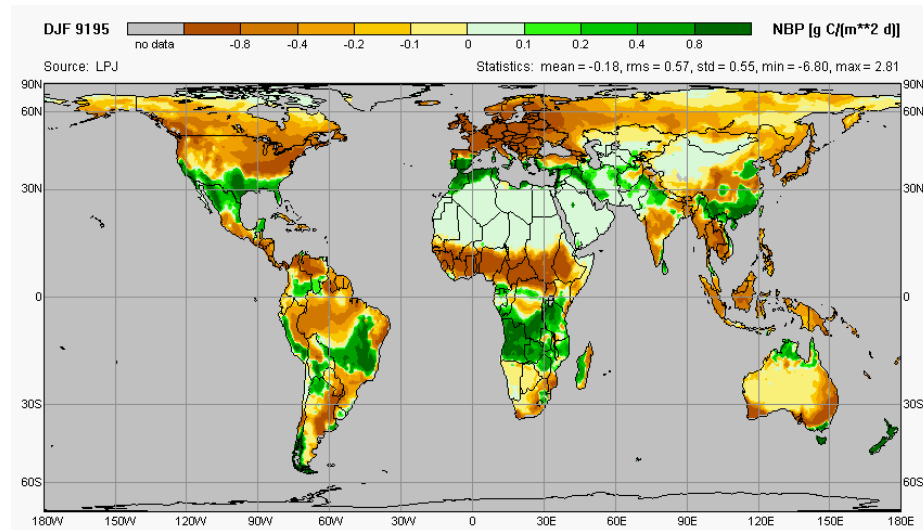


Gerten et al. (2005)

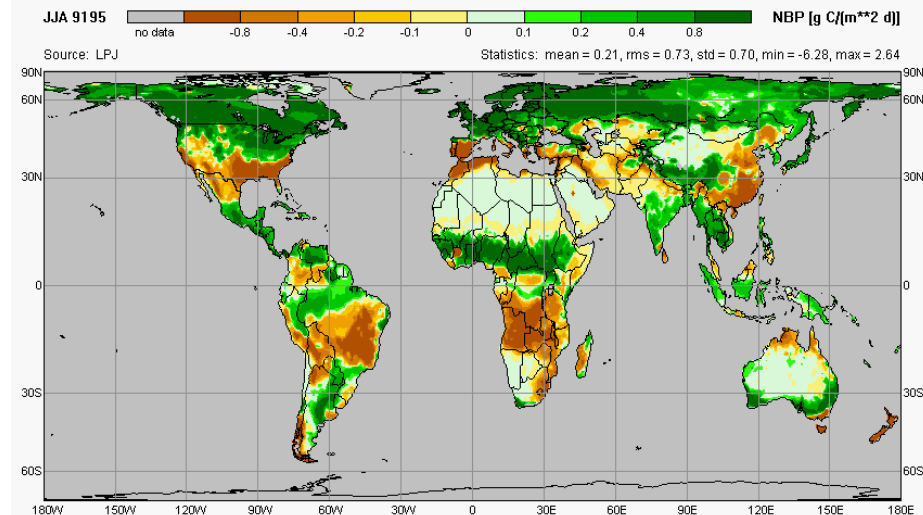
Calanca, 23.05.2006

# Worldwide distribution of NBP [g C m<sup>-2</sup> d<sup>-1</sup>]: seasonal mean values

Dec-Jan-Feb



Jun-Jul-Aug



Gerten et al. (2005)

# The radiative properties of foliage

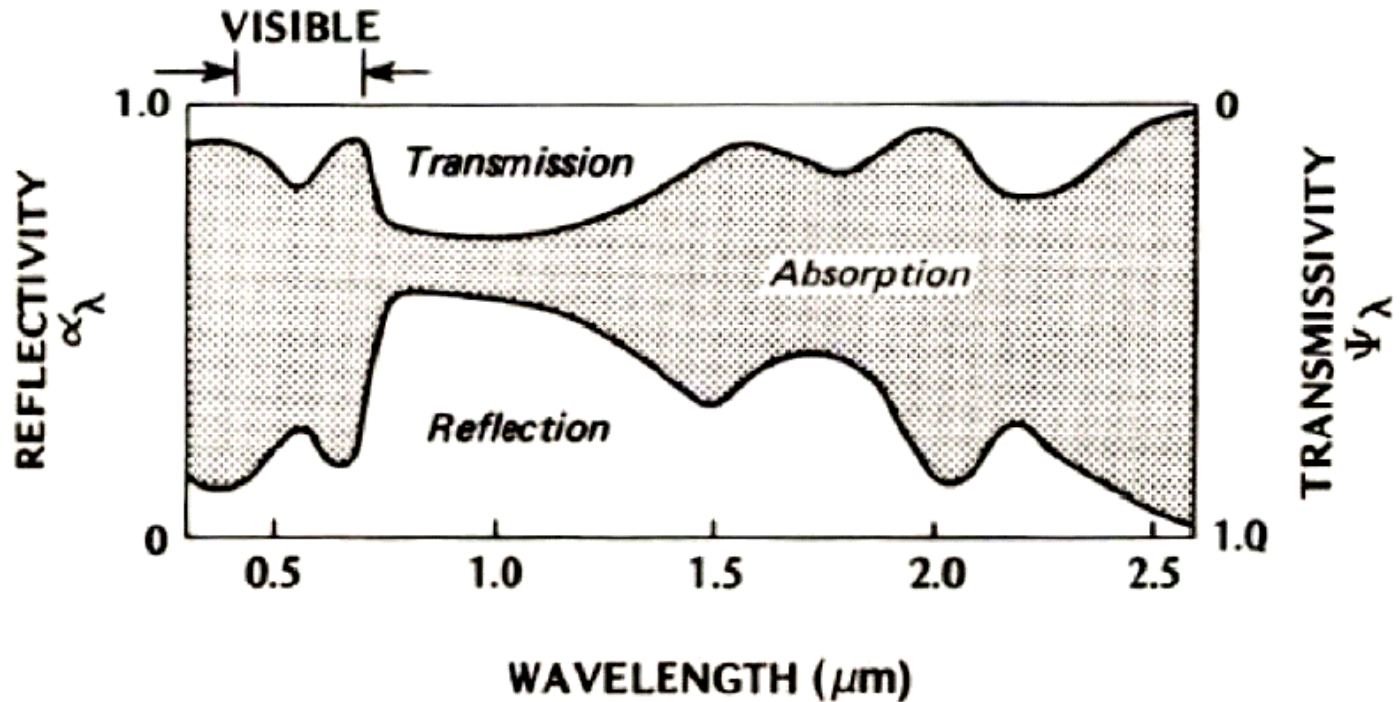


Figure 4.4 Idealized relation between wavelength and the reflectivity ( $\alpha$ ), transmissivity ( $\Psi$ ) and absorptivity ( $\zeta$ ) of a green leaf (after Monteith, 1965a).

Oke (1987)

# Photosynthetic Active Radiation (PAR)

Photosynthetic active radiation (PAR) is the part of the solar spectrum located between 0.4 and 0.7  $\mu\text{m}$  (400 to 700 nm). PAR is almost a constant fraction of global radiation (GI), and in the absence of specific measurements one can assume:

$$\text{PAR} \approx 0.47 \cdot \text{GI}$$

At noon (true solar time) under clear skies  $\text{GI} \sim 800 \text{ W m}^{-2}$  and the energy available for photosynthesis is  $\text{PAR} \sim 400 \text{ W m}^{-2}$ .

In ecological studies it is not uncommon to express PAR in units of  $\text{mol m}^{-2} \text{ s}^{-1}$ . To convert between  $[\text{W m}^{-2}]$  and  $[\text{mol m}^{-2} \text{ s}^{-1}]$  we need to know that:

- 1 quantum of radiation with frequency  $\nu$  has an energy in J equivalent to  $(h \nu)$ , where  $h = 6.63 \cdot 10^{-34} \text{ J s}$  is the Planck constant.
- The number of quanta in 1 mole of light is given by the Avogadro number  $N_A = 6.023 \cdot 10^{23} \text{ quanta mol}^{-1}$ .

As a rule of thumb,  $1 \text{ mol m}^{-2} \text{ s}^{-1} \approx 2 \cdot 10^5 \text{ W m}^{-2}$ .

# A global map of PAR

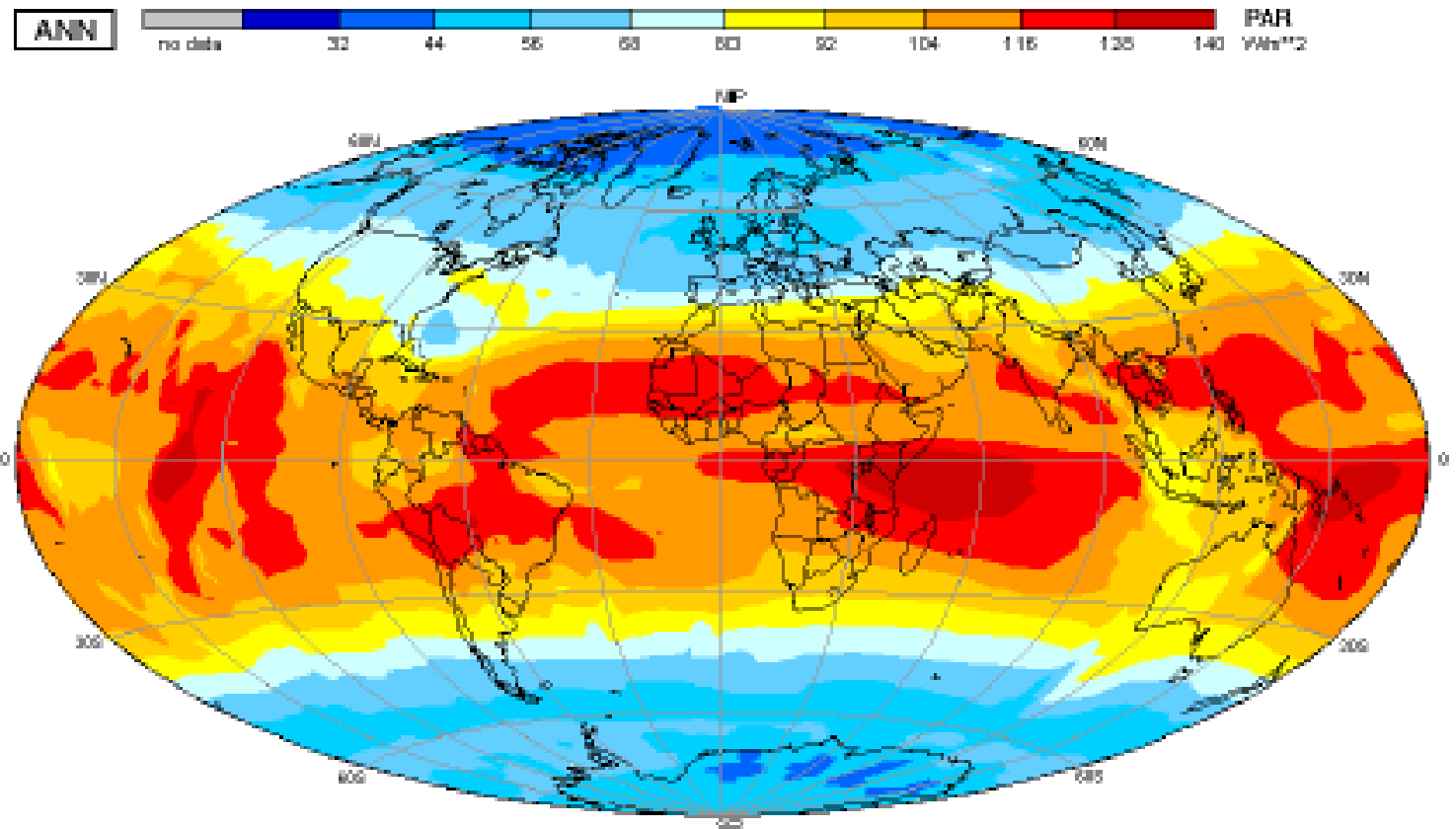


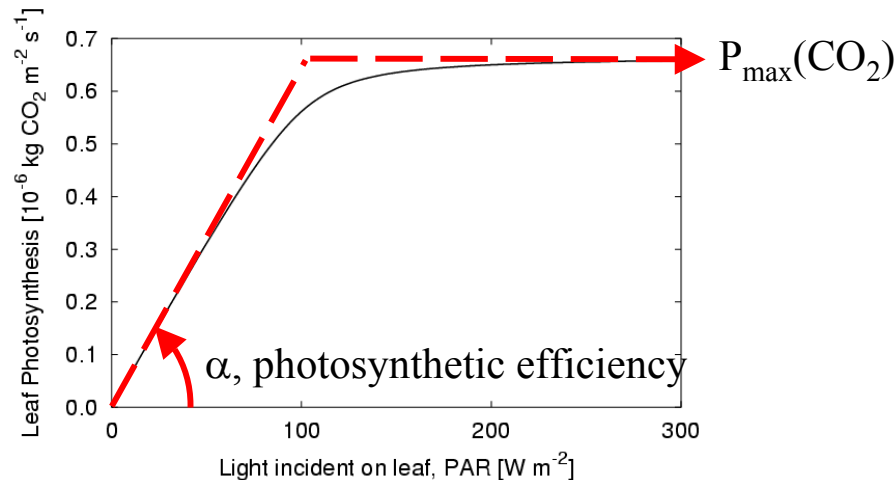
Fig. 4.4.1.1 A three-year climatology (1991 to 1993) of mean annual PAR (in  $\text{Wm}^{-2}$ ), which has been derived from ISCCP radiance data by (95Fro). This pattern is quite similar to that in the map for downward solar radiation. Errors at higher latitude might be higher than at lower latitudes. Due to the lack of a worldwide network of ground stations, an error limit can not be provided. Other definitions of the PAR use the photon flux density ( $\mu\text{mol s}^{-1} \text{cm}^{-2}$ ), where  $1 \text{ Wm}^{-2}$  may correspond to about 4.5 to  $5 \mu\text{mol s}^{-1} \text{cm}^{-2}$ .

# Leaf photosynthesis

Photosynthesis is the assimilation of atmospheric  $\text{CO}_2$  for reduction to carbohydrate. The assimilation of 1 kg  $\text{CO}_2$  requires  $\sim 10^7$  J PAR.

As far as climate is concerned, photosynthesis rate is limited either by radiation or atmospheric  $\text{CO}_2$  concentrations:

- at low radiances (intensities) leaf photosynthesis is directly proportional to the available PAR (radiation limited regime). The proportionality constant is the photosynthetic efficiency  $\alpha$ ;
- under conditions of light saturation, photosynthesis becomes proportional to the available  $\text{CO}_2$  ( $\text{CO}_2$  limited regime). In this regime one obtains the maximum rate of photosynthesis  $P_{\max}$  (for given  $\text{CO}_2$ ).

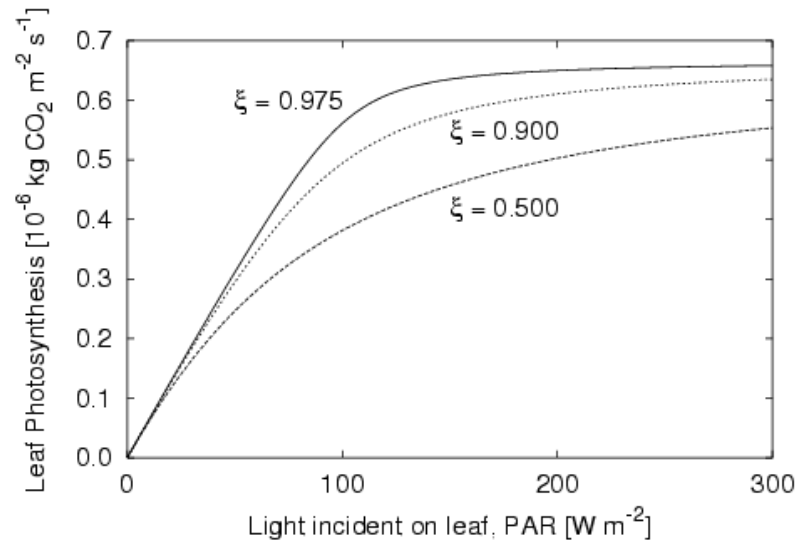


## Leaf photosynthesis (2)

A simple but flexible formula for describing leaf photosynthesis  $P_{\text{leaf}}$  that provides the correct asymptotic behaviour is the so-called non-rectangular hyperbola (Thornley and Johnson, 1990):

$$P_{\text{leaf}} = \frac{\alpha F_{\text{PAR}} + P_{\text{max}} - \sqrt{(\alpha F_{\text{PAR}} + P_{\text{max}})^2 - 4\xi\alpha F_{\text{PAR}} P_{\text{max}}}}{2\xi}$$

where  $F_{\text{PAR}}$  [ $\text{W m}^{-2}$ ] is the flux of PAR and  $\xi$  is a shape parameter determining the sharpness of the knee in the curve.



Thornley, J.H.M. and I.R. Johnson, 1990, *Plant and Crop Modelling*. Oxford University Press, Oxford, 669 pp.

# Canopy photosynthesis

Not all leaves in a canopy do assimilate CO<sub>2</sub> at the same rate. The two main reasons are:

- extinction of solar radiation in the canopy
- variations of CO<sub>2</sub> concentrations within the stand.

The extinction of solar radiation or PAR within the canopy can be describe using the Beer-Bouguer-Lambert law (see notes on ‘Radiative Transfer’) as:

$$F_{\text{PAR}}(z) = F_{\text{PAR}}(0)e^{-k_{\text{can}} \text{LAI}^*}$$

Here  $z$  is the depth below the canopy top,  $F_{\text{PAR}}$  the flux of solar radiation in the PAR range,  $k_{\text{can}} \sim 0.5 \text{ m}^2 \text{ ground (m}^2 \text{ leaf)}^{-1}$  the extinction coefficient of the canopy and  $\text{LAI}^*$ , in units of  $\text{m}^2 \text{ leaf (m}^2 \text{ ground)}^{-1}$ , the cumulative leaf-area index

# Within-canopy variations of climatic elements

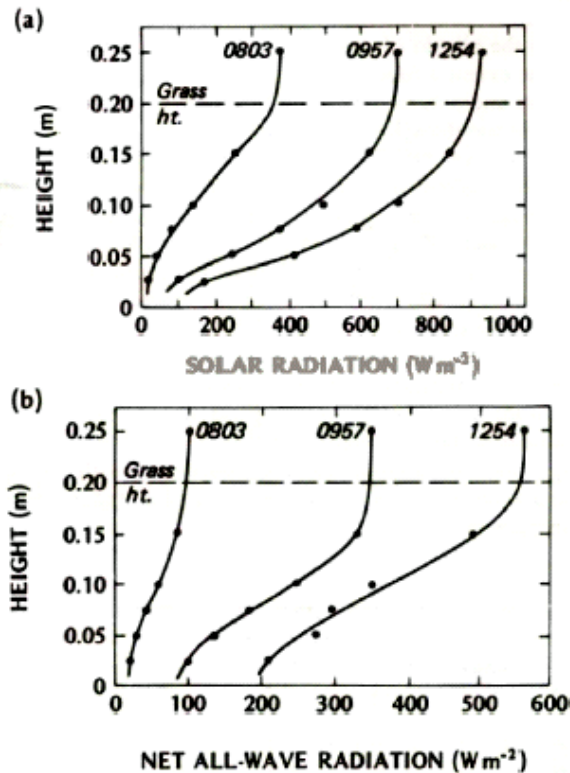


Figure 4.12 Measured profiles of (a) incoming solar ( $K \downarrow$ ), and (b) net all-wave radiation ( $Q^*$ ) in a 0.2 m stand of native grass at Matador, Sask., on 28 June 1972 (after Ripley and Redmann, 1976).

Oke (1987)

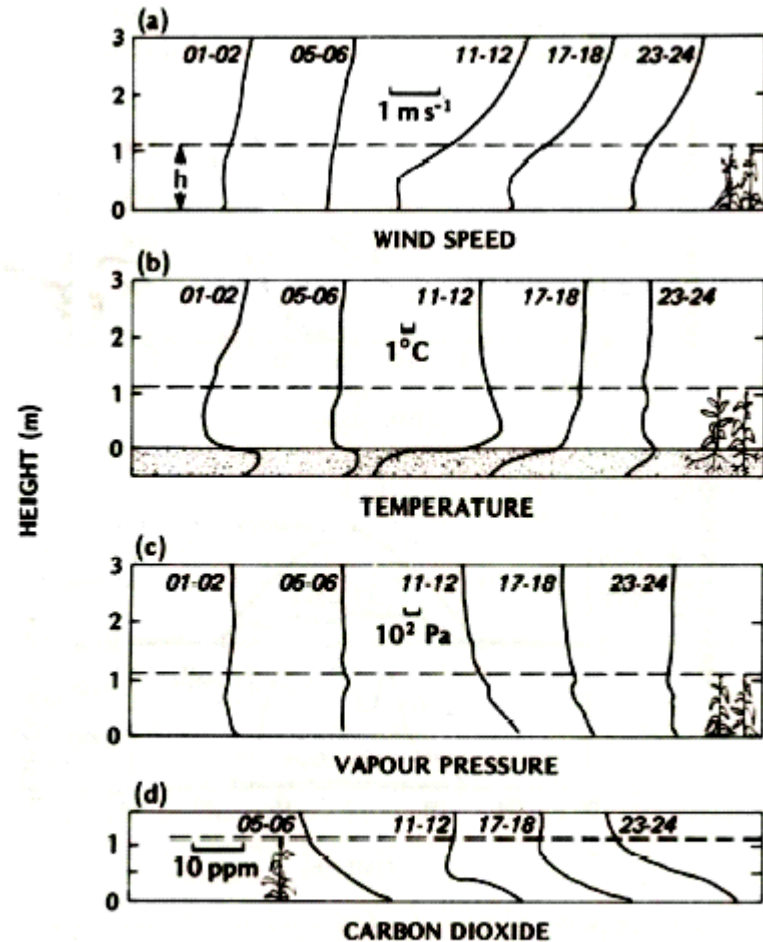


Figure 4.17 Profiles of (a) wind speed, (b) temperature, (c) vapour pressure and (d) carbon dioxide concentration in and above a barley field at Rothamsted, England on 23 July 1963 (modified after Long *et al.*, 1964).

# Monitoring GPP, NPP and NEP worldwide

A worldwide network of observing site, called FLUXNET, has been established at the beginning of the 1990s to monitor the net ecosystem exchange (NEE) of the terrestrial biosphere.

[Cart](#) [Sign In](#) [Register](#) [Tutorial](#) Quick Data Search  [Go](#)

[Home](#) [Project Info.](#) [Product Access](#) [Search Options](#) [Information](#) [Services](#)

**DAAC**  
for biogeochemical dynamics  
DISTRIBUTED ACTIVE ARCHIVE CENTER Oak Ridge National Laboratory

## FLUXNET Project

### Overview of the FLUXNET Project



FLUXNET is a global network of micrometeorological tower sites that use eddy covariance methods to measure the exchanges of carbon dioxide, water vapor, and energy between terrestrial ecosystem and atmosphere. At present, over 200 tower sites are operating on a long-term and continuous basis. Researchers also collect data on site vegetation, soil, hydrologic, and meteorological characteristics at the tower sites.

FLUXNET data available at the ORNL DAAC include monthly and annual heat, waper vapor, and carbon dioxide flux, gap-filled flux products, ecological site data, and remote-sensing products.

### FLUXNET Related Resources

Continue your exploration of the FLUXNET Project using the following on-line resources:

- [FLUXNET Data Set Documents](#)
- [FLUXNET Bibliography](#)

### Get FLUXNET Data

Find and order data sets:

- [See list of data sets](#)
- [Browse by attributes](#)

Use map server:

- [FLUXNET Map Server](#)

Download data sets directly:

- [FTP site](#)

### In-Depth

FLUXNET provides information to FLUXNET investigators and the public. The goals of FLUXNET are to understand the mechanisms controlling the exchanges of carbon dioxide, water vapor, and energy across a spectrum of time and space scales.

FLUXNET also provides ground information for validating estimates of net primary productivity, evaporation, and energy absorption that are being generated by sensors on the [NASA TERRA](#) satellite.

To read more, please visit our [FLUXNET Web Site](#)

### What's New at the DAAC?

LBA Radiance Data Released [Details...](#)

S2K MODIS Data Available [Details...](#)

LBA-ECO Data Set Available [Details...](#)

[Past announcements...](#)

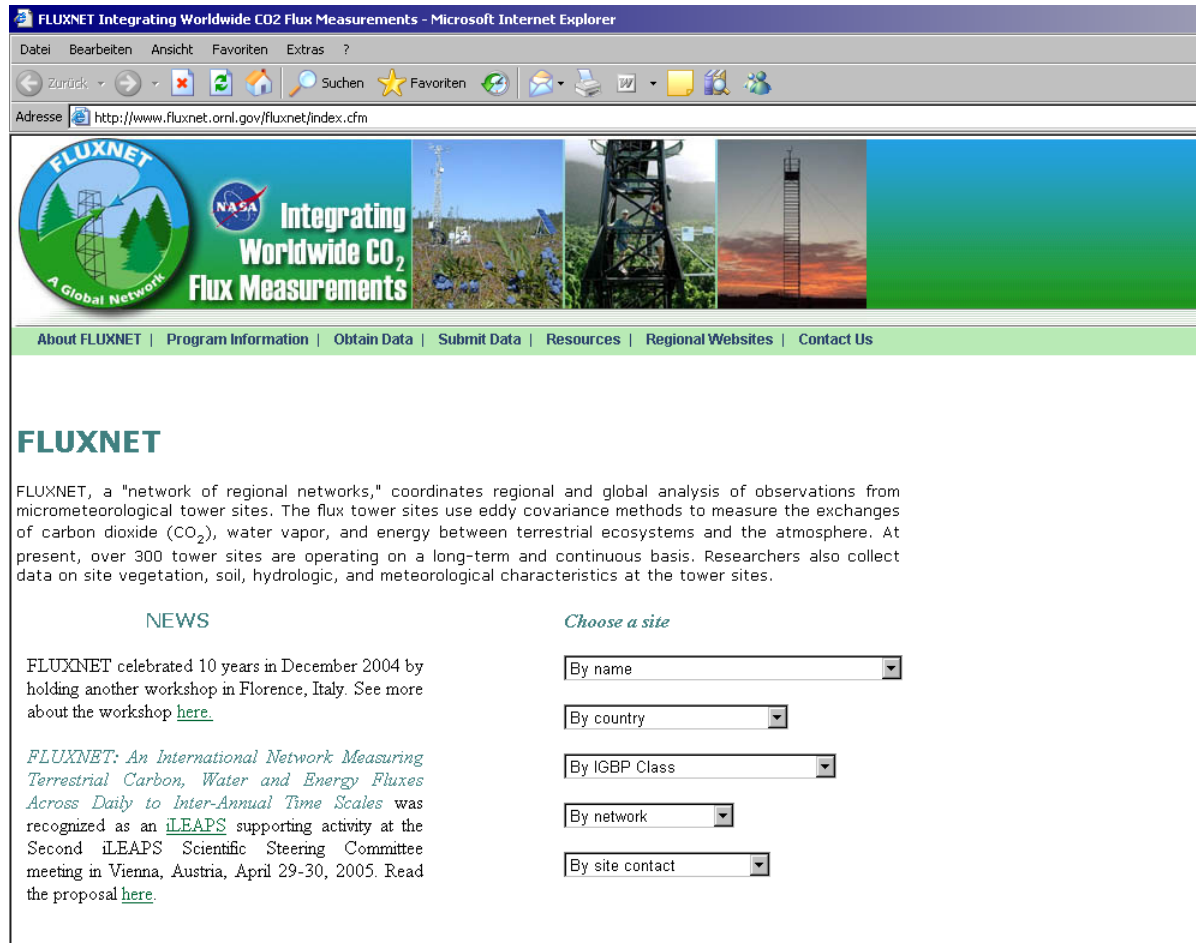
### Related Information

Web links to related information.

- [From the Ground Up \(2004\)](#) (pdf)
- [Earth Observatory: A View from Above](#)
- [ISLSCP Initiative II FLUXNET CO2 Measurements](#)
- [The Decade After Tomorrow, Modeling](#)

# FLUXNET

Informations about FLUXNET and its subprojects are provided on the internet.



FLUXNET Integrating Worldwide CO<sub>2</sub> Flux Measurements - Microsoft Internet Explorer

Adresse <http://www.fluxnet.ornl.gov/fluxnet/index.cfm>

**FLUXNET** Integrating Worldwide CO<sub>2</sub> Flux Measurements

[About FLUXNET](#) | [Program Information](#) | [Obtain Data](#) | [Submit Data](#) | [Resources](#) | [Regional Websites](#) | [Contact Us](#)

## FLUXNET

FLUXNET, a "network of regional networks," coordinates regional and global analysis of observations from micrometeorological tower sites. The flux tower sites use eddy covariance methods to measure the exchanges of carbon dioxide (CO<sub>2</sub>), water vapor, and energy between terrestrial ecosystems and the atmosphere. At present, over 300 tower sites are operating on a long-term and continuous basis. Researchers also collect data on site vegetation, soil, hydrologic, and meteorological characteristics at the tower sites.

### NEWS

FLUXNET celebrated 10 years in December 2004 by holding another workshop in Florence, Italy. See more about the workshop [here](#).

*FLUXNET: An International Network Measuring Terrestrial Carbon, Water and Energy Fluxes Across Daily to Inter-Annual Time Scales* was recognized as an iLEAPS supporting activity at the Second iLEAPS Scientific Steering Committee meeting in Vienna, Austria, April 29-30, 2005. Read the proposal [here](#).

*Choose a site*

By name

By country

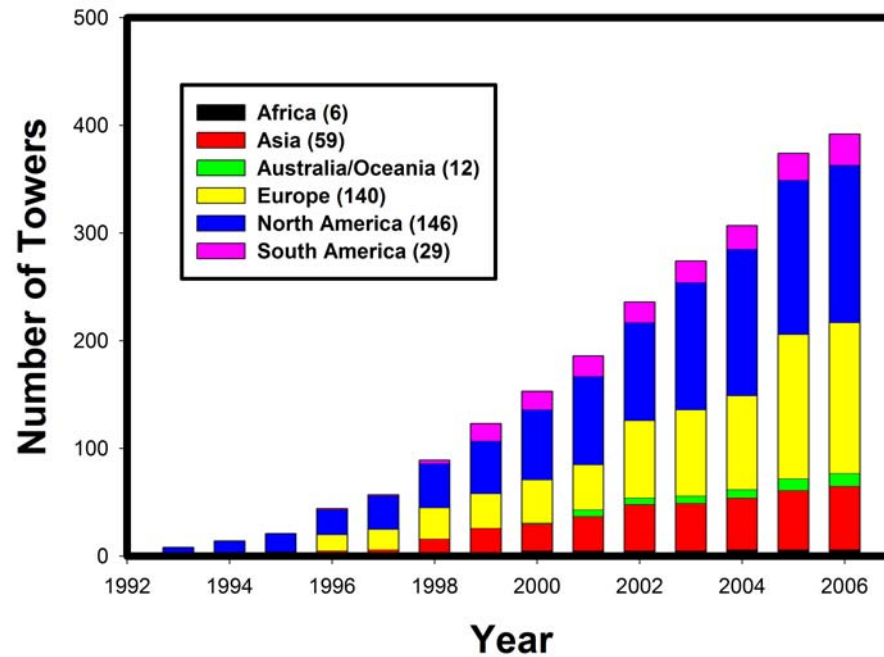
By IGBP Class

By network

By site contact

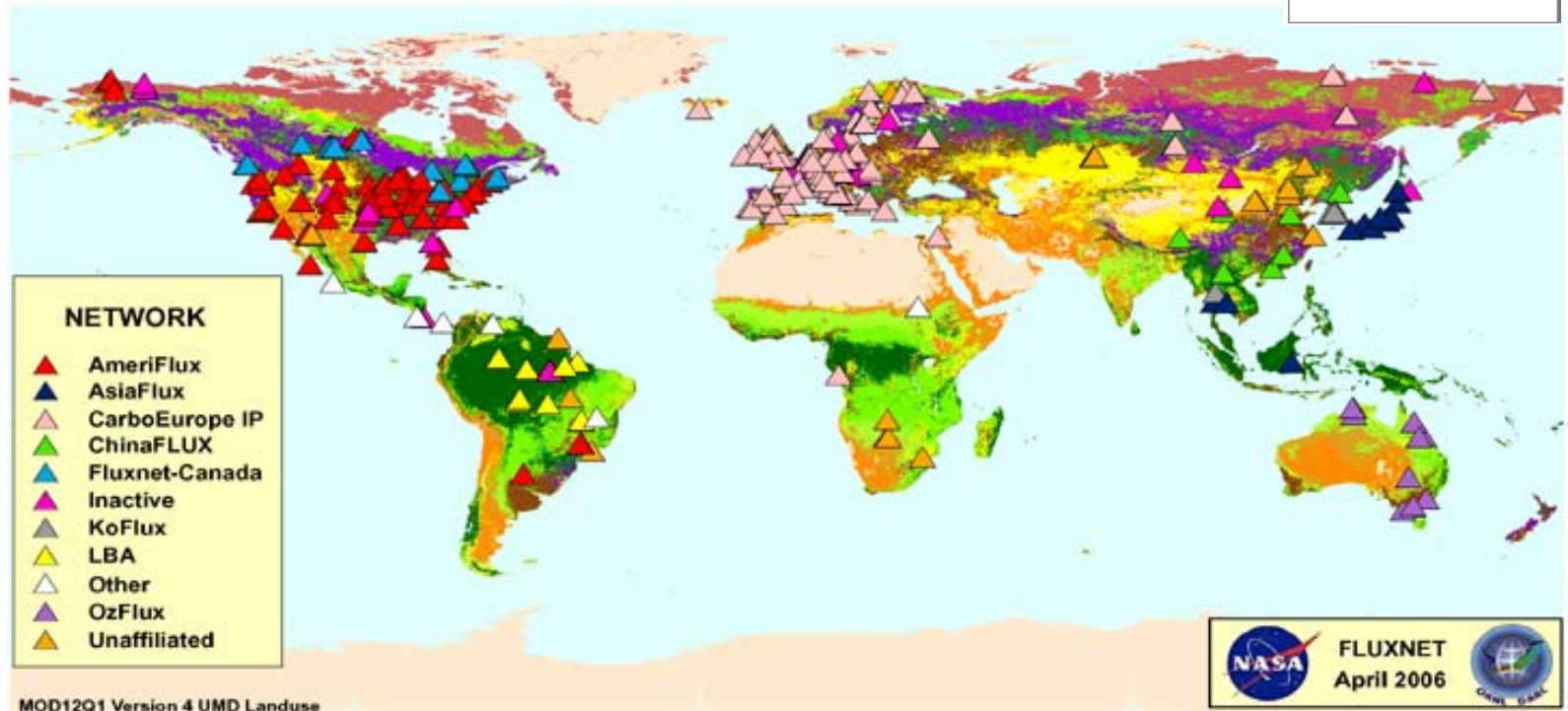
# FLUXNET (2)

## Growth of Fluxnet 406 Towers as of March 31, 2006



# FLUXNET (3)

Currently the exchange of CO<sub>2</sub> is measured at more than 200 sites (400 towers), covering all continents (except Antarctica) and a wide range of biogeographic conditions.



Legend to UMD Global Land Cover Classification map (source: Hansen, M., DeFries, R., Townshend, J. R. G. and Sohlberg, R., 2000, Global land cover classification at 1km resolution using a decision tree classifier, International Journal of Remote Sensing, 21: 1331-1365. DeFries, R., Hansen, M., Townshend, J. R. G. and Sohlberg, R., 1998, Global land cover classifications at 8 km spatial resolution: The use of training data derived from Landsat imagery in decision tree classifiers, International Journal of Remote Sensing, 19 (16): 3141-3168.). [\[More information on the University of Maryland Global Land Cover Facility\].](#)